



Title	Spin Current Generated from A Quantum Dot Driven by Pulsed Magnetic Resonance : Real-Time Spin Dynamics
Author(s)	Hattori, Kiminori
Citation	Journal of the Physical Society of Japan. 2010, 79(6), p. 064706
Version Type	AM
URL	<a href="https://hdl.handle.net/11094/3070">https://hdl.handle.net/11094/3070</a>
rights	
Note	

*The University of Osaka Institutional Knowledge Archive : OUKA*

<https://ir.library.osaka-u.ac.jp/>

The University of Osaka

# **Spin Current Generated from A Quantum Dot Driven by Pulsed Magnetic Resonance: Real-Time Spin Dynamics**

Kiminori HATTORI\*

*Department of Systems Innovation, Graduate School of Engineering Science, Osaka University,  
Toyonaka, Osaka 560-8531, Japan*

We investigate the real-time dynamics of spin current pumped from a quantum dot driven by pulsed magnetic resonance. Based on the nonequilibrium Green's function formalism, we obtain an exact solution to the time-dependent spin current occurring in such nonstationary situations. Performing numerical calculations, we demonstrate that a Rabi oscillation is exhibited in the transient spin current at the resonance, while the spin current eventually reaches its time-independent stationary value after a prolonged excitation. The spin current response in the time domain correlates directly to the time evolution of the spin state in the dot, suggesting the possibility of real-time spin measurement via pumped spin current.

**KEYWORDS:** spin pumping, spin current, quantum dot, magnetic resonance, real-time dynamics

\*E-mail: hattori@ee.es.osaka-u.ac.jp

## 1. Introduction

Extensive investigations have focused on the manipulation and measurement of electron spin in a mesoscopic quantum dot. These studies are motivated from the fine tunability of system parameters, easy preparation of a localized spin, and a long spin coherence time, all of which open up avenues for applications in spintronics and quantum information schemes.<sup>1-4)</sup> A primary element in this context is the ability to induce transitions between spin- $\uparrow$  and spin- $\downarrow$  states in a controlled way and to prepare arbitrary superpositions of these two basis states. This is commonly accomplished by magnetic resonance, in which an oscillating or equivalently rotating magnetic field resonantly couples two Zeeman levels in the presence of a static magnetic field. The coherent spin oscillation driven by magnetic resonance, and its measurement via charge current, have been demonstrated in quantum-dot systems theoretically<sup>5)</sup> and experimentally<sup>4)</sup>.

On the other hand, in the field of spintronics, which aims to exploit electron spin rather than charge in solid-state systems, a pure spin current composed of spin- $\uparrow$  and spin- $\downarrow$  electrons coherently moving in opposite directions without any net charge flow has attracted tremendous interest because of its intrinsically dissipationless nature.<sup>6-9)</sup> In particular, a quantum dot driven by magnetic resonance has been proposed as a generating source for stationary spin current.<sup>10-12)</sup> The spin-pumping mechanism is intuitively understood as follows. If the electrochemical potential is suitably positioned between the two spin levels in the dot, a spin- $\uparrow$  (spin- $\downarrow$ ) electron created by spin-flip transition is transferred into an infinitely extended reservoir coupled to the dot, leaving a hole which is subsequently filled with a spin- $\downarrow$  (spin- $\uparrow$ ) electron supplied by the reservoir. This process repeats to establish a continuous outgoing (incoming) flow of spin current in the steady-state.

In contrast to the stationary property of spin current, the time dependence of spin current is less studied, although the investigation of the temporal response to driving field is of prime importance for understanding spin generation and transport processes as well as their applications. In this paper, we address the real-time dynamics of spin current pumped from a quantum dot driven by pulsed magnetic resonance. An exact formulation for time-dependent spin current occurring in such nonstationary situations is derived using the nonequilibrium Green's function formalism. Numerical calculations implemented for a quantitative study of spin current dynamics reveal that a Rabi oscillation is exhibited in the transient spin current at the resonance while the spin current eventually becomes time-independent after a prolonged excitation. The spin current response in the time domain is basically explained in terms of the spin-current continuity equation as well as the spin Bloch equation, suggesting the possibility of spin measurement of the single dot via pumped spin current.

## 2. Theoretical Analysis and Formulation

Throughout this paper, we shall work in units where  $\hbar = e = k_B = 1$ . We consider a noninteracting single-level quantum dot subjected to a rotating transverse magnetic field  $\mathbf{B}_1(t) = B_1(t)(\mathbf{e}_x \cos \omega t + \mathbf{e}_y \sin \omega t)$  in addition to a static longitudinal magnetic field  $\mathbf{B}_0 = B_0 \mathbf{e}_z$ , where  $\mathbf{e}_{x,y,z}$  are unit vectors in Cartesian coordinates. Note that we allow the magnitude of the rotating field  $B_1(t)$  to vary in time. The Hamiltonian describing the dot is expressed as

$$H_d = \sum_{\sigma} \varepsilon_{d\sigma} d_{\sigma}^{\dagger} d_{\sigma} + \frac{\omega_1(t)}{2} \sum_{\sigma} d_{\sigma}^{\dagger} d_{-\sigma} e^{-i\sigma\omega t}, \quad (1a)$$

where  $d_{\sigma}$  denotes the annihilation operator for an electron with spin  $\sigma$  in the dot, and  $\varepsilon_{d\sigma} = \varepsilon_d + \sigma\omega_0/2$  is the spin-dependent particle energy in the absence of the rotating field. The

Zeeman interactions under the external fields are characterized by the Larmor frequencies  $\omega_{0,l} = \gamma B_{0,l}$ , where  $\gamma$  is the gyromagnetic ratio. For simplicity, the present model neglects electron-electron interaction in the dot. Spin pumping from the interacting dot is analyzed separately in Appendix A. The dot is coupled via tunneling to an infinitely extended reservoir, described by

$$H_r = \sum_{k\sigma} \varepsilon_{k\sigma} c_{k\sigma}^\dagger c_{k\sigma}, \quad (1b)$$

where  $c_{k\sigma}$  stands for the annihilation operator for an electron with momentum  $k$  and spin  $\sigma$  in the reservoir, and  $\varepsilon_{k\sigma} = \varepsilon_k + \sigma\omega_0/2$ . We assume a uniform static field spanning the reservoir region, and the same  $\gamma$  in the dot and the reservoir. This choice is not crucial for the following theoretical analysis. The identical formulation for spin pumping is derived (in the wideband limit) even for different Zeeman splittings. The coupling Hamiltonian reads

$$H_c = \sum_{k\sigma} (V_k d_\sigma^\dagger c_{k\sigma} + V_k^* c_{k\sigma}^\dagger d_\sigma), \quad (1c)$$

where the coupling coefficient  $V_k$  is assumed to be spin independent. The total Hamiltonian is thus modeled by the sum of these three contributions,  $H = H_d + H_r + H_c$ .

It is convenient to introduce the unitary transformation  $R(t) = \exp(i\omega t s_{tot}^z)$  with the total spin  $s_{tot}^z$  in the dot and the reservoir, which defines the Hamiltonian in the rotating reference frame as  $\tilde{H} = R(t)(H - i\partial_t)R^\dagger(t)$ .<sup>10,12,13)</sup> In the nonequilibrium Green's function formalism,<sup>14,15)</sup> we employ the retarded and lesser Green's functions defined by

$$G_{\sigma\sigma'}^+(t, t') = -i\langle \{d_\sigma(t), d_{\sigma'}^\dagger(t')\} \rangle \theta(t - t'), \quad (2a)$$

$$G_{\sigma\sigma'}^<(t, t') = i\langle d_{\sigma'}^\dagger(t') d_\sigma(t) \rangle, \quad (2b)$$

respectively. In the rotating frame, the retarded Green's function is described by

$$\tilde{G}^+(t, t') = -i\theta(t - t') e^{-\frac{\Gamma}{2}(t-t')} \mathcal{T} \exp[-i\int_{t'}^t dt_1 \tilde{H}_d(t_1)], \quad (3)$$

where  $\Gamma$  is the levelwidth due to the dot-reservoir coupling, and  $\mathcal{T}$  denotes the time-ordering operation. The Hamiltonian matrix is given by

$$\tilde{H}_d(t) = \begin{pmatrix} \tilde{\varepsilon}_{d\uparrow} & \frac{\omega_1(t)}{2} \\ \frac{\omega_1(t)}{2} & \tilde{\varepsilon}_{d\downarrow} \end{pmatrix},$$

where  $\tilde{\varepsilon}_{d\sigma} = \varepsilon_d + \sigma(\omega_0 - \omega)/2$ . The equal-time correlation function in the rotating frame is calculated to be

$$\tilde{G}_{\sigma\sigma'}^<(t, t) = i\Gamma \sum_{\rho} \int_{-\infty}^{\infty} \frac{d\varepsilon}{2\pi} f_{\rho}(\varepsilon) \tilde{A}_{\sigma\rho}(\varepsilon, t) \tilde{A}_{\rho\sigma'}^{\dagger}(\varepsilon, t), \quad (4)$$

where  $f_{\sigma}(\varepsilon) = f(\varepsilon + \sigma\omega/2)$  with  $f(\varepsilon)$  being the Fermi function in the reservoir, and the function  $\tilde{A}_{\sigma\sigma'}(\varepsilon, t)$  is defined by

$$\tilde{A}_{\sigma\sigma'}(\varepsilon, t) = \int_{-\infty}^{\infty} dt_1 e^{i\varepsilon(t-t_1)} \tilde{G}_{\sigma\sigma'}^{+, <}(t, t_1). \quad (5)$$

These results are also obtained from the nonequilibrium Green's functions in the laboratory frame (see Appendix B for details) via the general relation

$$G_{\sigma\sigma'}^{+, <}(t, t') = e^{-\frac{i}{2}\sigma\omega t} e^{\frac{i}{2}\sigma'\omega t'} \tilde{G}_{\sigma\sigma'}^{+, <}(t, t'), \quad (6)$$

between the two correlation functions in the laboratory and rotating frames.

The charge current consists of two contributions:  $J^c(t) = J_{out}^c(t) - J_{in}^c(t)$ , where  $J_{out}^c(t)$  describes the current flowing out from the dot, and  $J_{in}^c(t)$  concerns the current flowing into the dot.

Each component is represented as

$$J_{out}^c(t) = \Gamma N^c(t) = \Gamma^2 \sum_{\sigma\rho} \int_{-\infty}^{\infty} \frac{d\varepsilon}{2\pi} f_{\rho}(\varepsilon) \left| \tilde{A}_{\sigma\rho}(\varepsilon, t) \right|^2, \quad (7a)$$

$$J_{in}^c(t) = -\Gamma \sum_{\sigma} \int_{-\infty}^{\infty} \frac{d\varepsilon}{\pi} f_{\sigma}(\varepsilon) \text{Im} \tilde{A}_{\sigma\sigma}(\varepsilon, t), \quad (7b)$$

where  $N^c(t)$  denotes the dot charge. The classification into out- and in-currents is based on the property that  $J_{out}^c(t) > 0$  and  $\overline{J_{in}^c(t)} > 0$ , where the overbar denotes the time average. The latter

relation is easily shown from the charge-current continuity equation

$$\frac{d}{dt}N^c(t) + J^c(t) = 0. \quad (8)$$

Analogously, the spin current  $J^z(t) = J_{out}^z(t) - J_{in}^z(t)$  is expressed with

$$J_{out}^z(t) = \Gamma S^z(t) = \Gamma^2 \sum_{\sigma\rho} \sigma \int_{-\infty}^{\infty} \frac{d\varepsilon}{4\pi} f_{\rho}(\varepsilon) \left| \tilde{A}_{\sigma\rho}(\varepsilon, t) \right|^2, \quad (9a)$$

$$J_{in}^z(t) = -\Gamma \sum_{\sigma} \sigma \int_{-\infty}^{\infty} \frac{d\varepsilon}{2\pi} f_{\sigma}(\varepsilon) \text{Im} \tilde{A}_{\sigma\sigma}(\varepsilon, t), \quad (9b)$$

where  $S^z(t)$  denotes the dot spin. In eq. (9), we extend the terminology used for charge current to two distinctive components involved in spin current, although each component and its time average are not always positive. The spin-current continuity equation

$$\frac{d}{dt}S^z(t) + J^z(t) = G^z(t), \quad (10)$$

contains the spin torque contribution  $G^z(t)$ . In the rotating frame, the dot spin projected onto the  $xy$  plane is described by  $\tilde{S}^x(t) = \text{Im} \tilde{G}_{\uparrow\downarrow}^<(t, t)$  and  $\tilde{S}^y(t) = \text{Re} \tilde{G}_{\uparrow\downarrow}^<(t, t)$ . The out-of-plane spin torque is simply represented with  $\tilde{S}^y(t)$  as

$$G^z(t) = \omega_1(t) \tilde{S}^y(t). \quad (11)$$

Note that eq. (11) is identical to  $G^z(t) = [\tilde{\mathbf{\Omega}}(t) \times \tilde{\mathbf{S}}(t)]^z$ , where  $\tilde{\mathbf{\Omega}}(t) = (\omega_1(t) \ 0 \ \omega_0 - \omega)$  is the precession vector in the rotating frame.

Finally, we address applications of our general result to some particular cases. We first consider a continuous wave (CW) excitation, for which  $\omega_1(t) = \omega_1$  is time independent so that  $\tilde{A}(\varepsilon, t) = \tilde{G}^+(\varepsilon)$ . In this case, the dot Hamiltonian in the rotating frame is diagonalized with the rotation matrix  $\Theta_{\sigma\sigma'} = \cos \frac{\theta}{2} \delta_{\sigma\sigma'} + \sigma \sin \frac{\theta}{2} \delta_{\sigma, -\sigma'}$ , such that<sup>10,12)</sup>

$$\hat{H}_d = \Theta \tilde{H}_d \Theta^\dagger = \begin{pmatrix} \hat{\varepsilon}_{d\uparrow} & 0 \\ 0 & \hat{\varepsilon}_{d\downarrow} \end{pmatrix},$$

where  $\hat{\varepsilon}_{d\sigma} = \varepsilon_d + \sigma \tilde{\Omega}/2$  and  $\tan \theta = \omega_1/(\omega_0 - \omega)$ . The retarded Green's function  $\tilde{G}^+(\varepsilon)$  is

expressed as  $\tilde{G}^+(\varepsilon) = \Theta^\dagger \hat{G}^+(\varepsilon) \Theta$ , where  $\hat{G}_{\sigma\sigma'}^+(\varepsilon) = \delta_{\sigma\sigma'}(\varepsilon - \hat{\varepsilon}_{d\sigma} + i\Gamma/2)^{-1}$  is the retarded function defined in the transformed coordinates in which the  $z$ -axis points to the precession vector. Applying these analytical results to eq. (7) proves that  $J^c(t) = 0$ . In terms of eq. (8), the vanishing charge current is a natural consequence in stationary situations. On the other hand, eq. (9) predicts that the spin current is expressed as

$$J^z(t) = \Gamma^2 \int_{-\infty}^{\infty} \frac{d\varepsilon}{2\pi} [f_\downarrow(\varepsilon) - f_\uparrow(\varepsilon)] \left| \tilde{G}_{\uparrow\downarrow}^+(\varepsilon) \right|^2, \quad (12)$$

which is nonvanishing and time-independent. It is straightforward to show that eq. (12) reproduces the previous results for CW spin-pumping.<sup>11,12</sup> Next we proceed to a pulsed excitation described by

$$\omega_1(t) = \begin{cases} \omega_1, & t_0 < t \leq t_1, \\ 0, & \text{otherwise.} \end{cases}$$

Since the Hamiltonian matrix  $\tilde{H}_d(t)$  is time-independent within each time region separated by  $t_0$  and  $t_1$ , the time-ordered exponential contained in eq. (3) can be factorized into a product of ordinary exponentials. This feature allows us to easily handle the two-time propagator  $\tilde{G}^+(t, t')$ . Note that such a simplification is not possible for eq. (B.8) in the laboratory frame. Performing the time integration prescribed by eq. (5), we find a compact expression for  $\tilde{A}(\varepsilon, t)$ ,

$$\begin{cases} \tilde{A}_0(\varepsilon, t) = \tilde{G}^{+(0)}(\varepsilon), & t \leq t_0, \\ \tilde{A}_1(\varepsilon, t) = \Theta^\dagger \hat{\eta}(\varepsilon, t, t_0) \Theta \tilde{A}_0(\varepsilon, t_0) + \Theta^\dagger [1 - \hat{\eta}(\varepsilon, t, t_0)] \hat{G}^+(\varepsilon) \Theta, & t_0 < t \leq t_1, \\ \tilde{A}_2(\varepsilon, t) = \tilde{\eta}^{(0)}(\varepsilon, t, t_1) \tilde{A}_1(\varepsilon, t_1) + [1 - \tilde{\eta}^{(0)}(\varepsilon, t, t_1)] \tilde{G}^{+(0)}(\varepsilon), & t_1 < t, \end{cases} \quad (13)$$

with  $\hat{\eta}(\varepsilon, t, t') = i\hat{G}^+(t, t')e^{i\varepsilon(t-t')}$  and  $\tilde{\eta}^{(0)}(\varepsilon, t, t') = i\tilde{G}^{+(0)}(t, t')e^{i\varepsilon(t-t')}$ . Here, we use an auxiliary retarded function  $\tilde{G}_{\sigma\sigma'}^{+(0)}(\varepsilon) = \delta_{\sigma\sigma'}(\varepsilon - \tilde{\varepsilon}_{d\sigma} + i\Gamma/2)^{-1}$ , which corresponds to  $\tilde{G}_{\sigma\sigma'}^+(\varepsilon)$  for  $\omega_1 = 0$ . As is easily found, the CW result  $\tilde{A}(\varepsilon, t) = \tilde{G}^+(\varepsilon)$  is reasonably recovered when  $t_0 \rightarrow -\infty$  and  $t_1 \rightarrow +\infty$ . The time-dependent charge and spin currents for the pulsed excitation are numerically evaluated by plugging eq. (13) into eqs. (7) and (9).



### 3. Numerical Calculation and Discussion

In the rest of this paper, we discuss the numerical results for a pulsed excitation. In the following, the levelwidth  $\Gamma$  is taken as an energy unit ( $\Gamma = 1$ ). Correspondingly, the time unit becomes  $\Gamma^{-1}$ . The pulse starts at  $t = 0$  and ends at  $t = 6$ . The pulse duration  $\tau = 6$  is sufficiently long that the system nearly settles to its nonequilibrium steady-state under a continuous excitation. The Zeeman splitting is chosen to be as large as  $\omega_0 = 50$  so that the two spin levels are well separated from each other. We restrict our consideration to usual experimental situations where  $\omega_0 > \omega_1$ . All the results shown below are obtained at the resonant frequency  $\omega = \omega_0$ . In this case, the Rabi oscillation in a two-level system is expected to occur during the excitation. In the calculation, the dot level  $\varepsilon_d$  is assumed to be located at the Fermi level (in this case, the particle-hole symmetry is established) so that the dot always maintains single occupancy, i.e.,  $N^c(t) = 1$  and hence  $J^c(t) = 0$ . In this condition, we can explore the real-time dynamics of a pure spin current with no charge current.

Figure 1 displays the time-dependent spin current  $J^z(t)$  flowing out from the dot as a function of the excitation intensity  $\omega_1$  at zero temperature. Initially, the system remains in equilibrium, and no spin current is observed. After the excitation is turned on, the spin current abruptly increases and thereafter decays to its new steady-state value, which corresponds to the CW solution given by eq. (12). The steady-state spin current is independent of the excitation intensity  $\omega_1$  when  $\omega_1 > \Gamma$ . After the turnoff, the spin current decays exponentially back to zero. The exponential decay is simply characterized by the levelwidth  $\Gamma$ , which describes how fast an electron escapes from the dot. A most striking observation is a Rabi-type oscillation superposed

on the transient spin current. The spin-current oscillation occurs at the precession (or Rabi) frequency  $\tilde{\Omega} = \omega_1$  at resonance. The oscillation damps down exponentially at the rate  $\Gamma$ .

Figure 2 explains the spin dynamics in the rotating frame. The dot spin is initially polarized in the  $-z$  direction under the static field. After the excitation is turned on, the spin vector  $\tilde{\mathbf{S}}(t)$  rotates around the precession vector  $\tilde{\mathbf{\Omega}} = (\omega_1 \ 0 \ 0)$  at the resonance. Reflecting the spin rotation,  $\tilde{S}^{y,z}(t)$  oscillate with time while  $\tilde{S}^x(t)$  remains around zero. Note that the projections onto the  $z$ -axis are identical in the laboratory and rotating frames, i.e.,  $S^z(t) = \tilde{S}^z(t)$ . For a sufficiently prolonged excitation,  $\tilde{S}^y(t)$  decays but remains finite whereas  $S^z(t)$  goes to zero. The spin torque  $G^z(t)$  directly relates to  $\tilde{S}^y(t)$ , as explicitly indicated in eq. (11). Therefore, the nonzero  $\tilde{S}^y$  occurring in the steady state accounts for the CW spin pumping, for which  $J^z = G^z$  in terms of eq. (10). After the turnoff,  $\tilde{\mathbf{S}}(t)$  eventually returns to its equilibrium value. The spin relaxation time is isotropic in the present model, and is simply characterized by  $\Gamma^{-1}$ .

The spin-current continuity equation, eq. (10), holds exactly in the numerical results. Figure 3 (a) shows its components,  $dS^z/dt$ ,  $J^z(t)$ , and  $G^z(t)$ , separately. Just before the turnoff,  $dS^z/dt \cong 0$  since  $S^z(t)$  approaches its steady-state value. As a result, the relation  $J^z(t) \cong G^z(t)$  is established. After the turnoff,  $G^z(t) = 0$  so that  $J^z(t) = -dS^z/dt$ , indicating that in this time region, the nonequilibrium excess spin accumulated on the dot is released into the reservoir. Figure 3 (b) displays the out- and in-current components involved in the pumped spin current  $J^z(t) = J_{out}^z(t) - J_{in}^z(t)$ . Remarkably, the in-current component  $J_{in}^z(t)$  is almost time-independent over the entire time range. This feature is commonly observed for  $\omega = \omega_0 > \omega_1$ .

From these observations, a close correlation is expected between the time-dependent spin current and the time-dependent spin state in the dot. The equation of motion for the dot spin can be derived from the Kadanoff-Baym formulation of nonequilibrium Green's functions, in which we

address integro-differential equations.<sup>15)</sup> This method is mathematically equivalent to the Keldysh formulation employed for analyzing the time-dependent spin current in the preceding section, in which we deal with integral equations. The results are cast into a Bloch-type equation<sup>16)</sup>

$$\frac{d}{dt}\mathbf{S}(t) = \mathbf{\Omega}(t) \times \mathbf{S}(t) - \mathbf{R}(t). \quad (14)$$

It is immediately noticed that in regard to the  $z$ -projection, the Bloch equation, eq. (14), is structurally equivalent to the spin-current continuity equation, eq. (10). As described above,  $J_{in}^z(t)$  is independent of time in usual situations where  $\omega = \omega_0 > \omega_1$ . Obviously, the in-current component should obey  $J_{in}^z = \Gamma S_{eq}^z$  in thermal equilibrium. Consequently, we arrive at the important conclusion that  $J^z(t) = R^z(t) = \Gamma[S^z(t) - S_{eq}^z]$ , showing that the time evolution of the dot spin is monitored by the spin current pumped from the dot. Thus, spin pumping naturally constitutes a spin measurement (or readout) process. The output spin current can be detected electrically, e.g., by exploiting the inverse spin-Hall effect whereby a spin current is converted into a transverse charge imbalance (and a Hall voltage).<sup>17-20)</sup> On the other hand, the identity  $J^z(t) = R^z(t)$  implies an underlying Zeno effect, i.e., a coherent Rabi oscillation tends to be suppressed by a strong coupling to the reservoir for extracting a large spin current.

Finally, we explain briefly the temperature dependence of pumped spin current. Figure 4 illustrates that the spin current  $J^z(t)$  remains unchanged at low temperatures while it monotonically decreases in magnitude with increasing temperature  $T$  when  $T > \omega_0/2$ . However, the fringe visibility of Rabi oscillation in  $J^z(t)$  is essentially temperature-independent. Actually,  $J^z(t, T)$  is logarithmically shifted with  $T$ . As demonstrated in Fig. 5, the temporal spin information of the dot is probed via spin current even at high temperatures as well.

#### 4. Summary

The real-time dynamics of spin current pumped from a quantum dot driven by pulsed magnetic resonance have been investigated using the nonequilibrium Green's function formalism. In the wideband limit, an exact formulation was derived for the time-dependent spin current occurring in nonstationary situations. Numerical calculation based on the theoretical result was implemented for a quantitative study of spin current response to a burst of a rotating field. The transient spin current was found to exhibit a Rabi oscillation due to the resonance with the driving field, while the spin current eventually becomes time-independent after a prolonged excitation. The spin current dynamics are explained in terms of the spin-current continuity equation, or equivalently, the spin Bloch equation, including the spin torque exerted on the dot as the driving term and the spin current flowing out from the dot as the relaxation term. The time-dependent spin current reflects the time evolution of the dot spin, enabling a spin measurement in the time domain.

### **Acknowledgement**

This work was supported by a Grant-in-Aid for Scientific Research (No. 21540320) from the Japan Society for the Promotion of Science.

## Appendix A: Coulomb Interaction

In this appendix, we explain spin pumping from a quantum dot in which a strong Coulomb interaction  $U$  exists between two electrons. The dynamics of an interacting dot coupled to a macroscopic reservoir may be described by a reduced density matrix, which is defined by tracing out the reservoir variables in the total density matrix. Assuming the infinite Coulomb interaction ( $U \rightarrow \infty$ ) and the Fermi level located between two Zeeman levels, the equation of motion for the reduced density matrix  $\rho$  is formulated within the Born-Markov approximation as

$$\frac{d}{dt}\rho_{00}(t) = \Gamma[\rho_{\uparrow\uparrow}(t) - \rho_{00}(t)],$$

$$\frac{d}{dt}\rho_{\uparrow\uparrow}(t) = -\omega_1(t)\text{Im}[e^{i\omega t}\rho_{\uparrow\downarrow}(t)] - \Gamma\rho_{\uparrow\uparrow}(t),$$

$$\frac{d}{dt}\rho_{\downarrow\downarrow}(t) = \omega_1(t)\text{Im}[e^{i\omega t}\rho_{\uparrow\downarrow}(t)] + \Gamma\rho_{00}(t),$$

$$\frac{d}{dt}\rho_{\uparrow\downarrow}(t) = -i\omega_0\rho_{\uparrow\downarrow}(t) + \frac{i\omega_1(t)}{2}e^{-i\omega t}[\rho_{\uparrow\uparrow}(t) - \rho_{\downarrow\downarrow}(t)] - \frac{\Gamma}{2}\rho_{\uparrow\downarrow}(t),$$

at zero temperature.<sup>5,21,22</sup> Note that double occupation is prohibited so that there are only three available states:  $|0\rangle$  (empty dot),  $|\uparrow\rangle$  (dot occupied with a spin- $\uparrow$  electron), and  $|\downarrow\rangle$  (the same with a spin- $\downarrow$  electron). In terms of the density matrix, the charge and spin currents flowing out from the dot are simply expressed as  $J^c = \Gamma(\rho_{\uparrow\uparrow} - \rho_{00})$  and  $J^z = \Gamma(\rho_{\uparrow\uparrow} + \rho_{00})/2$ , respectively. The numerical solution for pulsed excitation is illustrated in Fig. A.1. The pumped spin current exhibits the Rabi oscillation, while in this case, the nonzero charge current occurs because of the elimination of double occupancy and the resulting particle-hole asymmetry. The time-dependent charge and spin currents contain the information on the time evolution of the system. Particularly, the diagonal elements of density matrix,  $\rho_{00}$ ,  $\rho_{\uparrow\uparrow}$ , and  $\rho_{\downarrow\downarrow} = 1 - \rho_{00} - \rho_{\uparrow\uparrow}$ , can be directly evaluated from  $J^c$  and  $J^z$ , enabling a simultaneous measurement of the dot charge

$N^c = \rho_{\uparrow\uparrow} + \rho_{\downarrow\downarrow}$  and the dot spin  $S^z = (\rho_{\uparrow\uparrow} - \rho_{\downarrow\downarrow})/2$ . It is also worth noting that the direct correlation between  $\rho$  and  $J^{c,z}$  is not affected by a possible intrinsic spin decoherence due to hyperfine interaction, spin-orbit coupling, etc.

## Appendix B: Laboratory Frame

In this appendix, we describe the theoretical formulation based on the nonequilibrium Green's functions in the laboratory frame. Before going into a detailed theoretical analysis, it may be worth explaining that the underlying physics of spin pumping can be captured at the operator level. It is straightforward to show that the Heisenberg equations for number operators  $n_{d\sigma}(t) = d_{\sigma}^{\dagger}(t)d_{\sigma}(t)$  and  $n_{r\sigma}(t) = \sum_k c_{k\sigma}^{\dagger}(t)c_{k\sigma}(t)$  lead to the standard continuity equation for charge current  $dn^c/dt + j^c(t) = 0$ , where  $n^c(t) = \sum_{\sigma} n_{d\sigma}(t)$  is the dot charge, and  $j^c(t) = \frac{d}{dt} \sum_{\sigma} n_{r\sigma}(t)$  is the charge current flowing in the reservoir. The continuity equation is written in a sourceless form owing to charge conservation. The situation is different for spin current because spin conservation is violated in the presence of the rotating field. The continuity equation for spin current is formulated in a similar manner as  $ds^z/dt + j^z(t) = g^z(t)$ , where  $s^z(t) = \frac{1}{2} \sum_{\sigma} \sigma n_{d\sigma}(t)$  is the dot spin, and  $j^z(t) = \frac{1}{2} \frac{d}{dt} \sum_{\sigma} \sigma n_{r\sigma}(t)$  is the spin current flowing in the reservoir. The spin torque operator  $g^z(t) = \frac{\omega_1(t)}{2i} \sum_{\sigma} \sigma d_{\sigma}^{\dagger}(t)d_{-\sigma}(t)e^{-i\sigma\omega t}$  appearing as a source term accounts for spin generation due to the rotating field. It is easily found that the spin torque may be expressed as  $g^z(t) = [\mathbf{\Omega}(t) \times \mathbf{s}(t)]^z$  with the angular velocity of Larmor precession  $\mathbf{\Omega}(t) = (\omega_1(t)\cos\omega t \quad \omega_1(t)\sin\omega t \quad \omega_0)$ .

We begin our analysis with the general expression for the time-dependent particle current

$$J_{\sigma}(t) = \frac{d}{dt} \langle n_{r\sigma}(t) \rangle = -2\text{Re} \int_{-\infty}^{\infty} dt_1 [G_{\sigma\sigma}^{+}(t, t_1) \Sigma_{\sigma}^{<}(t_1, t) + G_{\sigma\sigma}^{<}(t, t_1) \Sigma_{\sigma}^{-}(t_1, t)], \quad (\text{B} \cdot 1)$$

where  $\Sigma_{\sigma}^{<-}(t, t') = \sum_k |V_k|^2 g_{k\sigma}^{<-}(t, t')$  are the lesser and advanced self-energies, respectively. The Green's functions of the reservoir  $g_{k\sigma}^{<-}(t, t')$  are explicitly written as  $g_{k\sigma}^{<-}(t, t') = if(\varepsilon_{k\sigma})e^{-i\varepsilon_{k\sigma}(t-t')}$  and  $g_{k\sigma}^{>-}(t, t') = ie^{-i\varepsilon_{k\sigma}(t-t')}\theta(t' - t)$ , where  $f(\varepsilon)$  is the Fermi function in the reservoir. In energy representation, eq. (B.1) becomes

$$J_{\sigma}(t) = \text{Im} \int_{-\infty}^t dt_1 \int_{-\infty}^{\infty} \frac{d\varepsilon}{\pi} e^{i\varepsilon(t-t_1)} \Gamma(\varepsilon - \frac{\sigma\omega_0}{2}) [G_{\sigma\sigma}^{+}(t, t_1)f(\varepsilon) + G_{\sigma\sigma}^{<-}(t, t_1)],$$

where  $\Gamma(\varepsilon) = 2\pi\rho(\varepsilon)|V(\varepsilon)|^2$  is the linewidth function, and  $\rho(\varepsilon) = \sum_k \delta(\varepsilon - \varepsilon_k)$  is the density of states per spin in the reservoir. To simplify discussion, we adopt the wideband limit where  $\Gamma$  is taken to be independent of energy. In this case, the above expression is reduced to

$$J_{\sigma}(t) = \Gamma \int_{-\infty}^{\infty} \frac{d\varepsilon}{\pi} f(\varepsilon) \text{Im} A_{\sigma\sigma}(\varepsilon, t) + \Gamma N_{\sigma}(t), \quad (\text{B.2})$$

where  $N_{\sigma}(t) = \langle n_{d\sigma}(t) \rangle = -iG_{\sigma\sigma}^{<-}(t, t)$  is the dot occupation number, and the function  $A_{\sigma\sigma}(\varepsilon, t)$  is defined by

$$A_{\sigma\sigma'}(\varepsilon, t) = \int_{-\infty}^{\infty} dt_1 e^{i\varepsilon(t-t_1)} G_{\sigma\sigma'}^{+}(t, t_1). \quad (\text{B.3})$$

In stationary situations,  $G_{\sigma\sigma'}^{+}(t, t')$  depends only on the time difference  $t - t'$ , and thereby  $A_{\sigma\sigma'}(\varepsilon)$  simply coincides with the Fourier transform of the retarded Green's function  $G_{\sigma\sigma'}^{+}(\varepsilon)$ . However, this is not what we address. It must be borne in mind that here we deal with the time-dependent case so that  $G_{\sigma\sigma'}^{+}(t, t')$  as well as  $G_{\sigma\sigma'}^{<-}(t, t')$  depend on the two time variables separately. The lesser Green's function obeys the Keldysh equation, expressed generally as

$$G^{<-}(t, t') = \int_{-\infty}^{\infty} dt_1 dt_2 G^{+}(t, t_1) \Sigma^{<-}(t_1, t_2) G^{-}(t_2, t'), \quad (\text{B.4})$$

in matrix notation. Applying the wideband approximation, the equal-time correlation function is formulated as

$$G^{<-}(t, t) = i\Gamma \int_{-\infty}^{\infty} \frac{d\varepsilon}{2\pi} f(\varepsilon) A(\varepsilon, t) A^{\dagger}(\varepsilon, t), \quad (\text{B.5})$$

in terms of  $A(\varepsilon, t)$ , and hence the dot occupation number is given by

$$N_\sigma(t) = \Gamma \sum_\rho \int_{-\infty}^{\infty} \frac{d\varepsilon}{2\pi} f(\varepsilon) \left| A_{\sigma\rho}(\varepsilon, t) \right|^2. \quad (\text{B.6})$$

Thus the whole knowledge of the time evolution of the system is contained in  $A(\varepsilon, t)$  or equivalently  $G^+(t, t')$ . In the wideband limit, the retarded Green's function obeys the equation of motion

$$\left[ i \frac{\partial}{\partial t} - H_d(t) + \frac{i\Gamma}{2} \right] G^+(t, t') = \delta(t - t'), \quad (\text{B.7})$$

where the time-dependent matrix

$$H_d(t) = \begin{pmatrix} \varepsilon_{d\uparrow} & \frac{\omega_1(t)}{2} e^{-i\omega t} \\ \frac{\omega_1(t)}{2} e^{i\omega t} & \varepsilon_{d\downarrow} \end{pmatrix},$$

represents the dot Hamiltonian. The solution is easily found to be

$$G^+(t, t') = -i\theta(t - t') e^{-\frac{\Gamma}{2}(t-t')} \mathcal{T} \exp[-i \int_{t'}^t dt_1 H_d(t_1)]. \quad (\text{B.8})$$



## REFERENCES

- 1) D. Loss and D. P. DiVincenzo: Phys. Rev. A **57** (1998) 120.
- 2) J. M. Elzerman, R. Hanson, L. H. Willems van Beveren, B. Witkamp, L. M. K. Vandersypen, and L. P. Kouwenhoven: Nature (London) **430** (2004) 431.
- 3) J. R. Petta, A. C. Johnson, J. M. Taylor, E. A. Laird, A. Yacoby, M. D. Lukin, C. M. Marcus, M. P. Hanson, and A. C. Gossard: Science **309** (2005) 2180.
- 4) F. H. L. Koppens, C. Buizert, K. J. Tielrooij, I. T. Vink, K. C. Nowack, T. Meunier, L. P. Kouwenhoven, and L. M. K. Vandersypen: Nature (London) **442** (2006) 766.
- 5) H.-A. Engel and D. Loss: Phys. Rev. Lett. **86** (2001) 4648.
- 6) M. J. Stevens, A. L. Smirl, R. D. R. Bhat, A. Najmaie, J. E. Sipe, and H. M. van Driel: Phys. Rev. Lett. **90** (2003) 136603.
- 7) S. Murakami, N. Nagaosa, and S.-C. Zhang: Phys. Rev. B **69** (2004) 235206.
- 8) J. Sinova, D. Culcer, Q. Niu, N. A. Sinitsyn, T. Jungwirth, and A. H. MacDonald: Phys. Rev. Lett. **92** (2004) 126603.
- 9) N. Nagaosa: J. Phys. Soc. Jpn. **77** (2008) 031010.
- 10) P. Zhang, Q.-K. Xue, and X. C. Xie: Phys. Rev. Lett. **91** (2003) 196602.
- 11) B. Wang, J. Wang, and H. Guo: Phys. Rev. B **67** (2003) 092408.
- 12) K. Hattori: Phys. Rev. B **78** (2008) 155321.
- 13) K. Hattori: Phys. Rev. B **75** (2007) 205302.
- 14) A.-P. Jauho, N. S. Wingreen, and Y. Meir: Phys. Rev. B **50** (1994) 5528.
- 15) H. Haug and A.-P. Jauho: *Quantum Kinetics in Transport and Optics of Semiconductors* (Springer-Verlag, New York, 2007).

16) Following the nonequilibrium Green's function formalism, one finds that

$$R^x(t) = \Gamma \sum_{\sigma} \int_{-\infty}^{\infty} \frac{d\varepsilon}{2\pi} f(\varepsilon) \text{Im} A_{\sigma,-\sigma}(\varepsilon, t) + \Gamma S^x(t), \quad R^y(t) = \Gamma \sum_{\sigma} \sigma \int_{-\infty}^{\infty} \frac{d\varepsilon}{2\pi} f(\varepsilon) \text{Re} A_{\sigma,-\sigma}(\varepsilon, t) + \Gamma S^y(t),$$

$$\text{and } R^z(t) = \Gamma \sum_{\sigma} \sigma \int_{-\infty}^{\infty} \frac{d\varepsilon}{2\pi} f(\varepsilon) \text{Im} A_{\sigma\sigma}(\varepsilon, t) + \Gamma S^z(t).$$

17) J. E. Hirsch: Phys. Rev. Lett. **83** (1999) 1834.

18) S. O. Valenzuela and M. Tinkham: Nature (London) **442** (2006) 176.

19) E. Saitoh, M. Ueda, H. Miyajima, and G. Tatara: Appl. Phys. Lett. **88** (2006) 182509.

20) T. Kimura, Y. Otani, T. Sato, S. Takahashi, and S. Maekawa: Phys. Rev. Lett. **98** (2007) 156601.

21) K. Blum: *Density Matrix Theory and Applications* (Plenum, New York, 1996).

22) I. Martin, D. Mozyrsky, and H. W. Jiang: Phys. Rev. Lett. **90** (2003) 018301.

## FIGURE CAPTIONS

FIG. 1

(Color online) Time-dependent spin current  $J^z(t)$  as a function of excitation intensity  $\omega_1$  at zero temperature. The excitation pulse length is set at  $\tau = 6$ . The parameters used in the calculation are  $\omega = \omega_0 = 50$ .

FIG. 2

(Color online) Time evolution of dot spin  $\tilde{\mathbf{S}}(t) = (\tilde{S}^x(t) \ \tilde{S}^y(t) \ S^z(t))$  in the rotating frame (a) and its trajectory projected onto the  $yz$  plane (b). The  $z$ -projections are identical in the laboratory and rotating frames ( $S^z = \tilde{S}^z$ ). The vertical lines in (a) indicate the duration of the excitation pulse. The parameters used in the calculation are  $\omega = \omega_0 = 50$  and  $\omega_1 = 10$ .

FIG. 3

(Color online) (a) Spin current  $J^z(t)$ , spin torque  $G^z(t)$ , and time-derivative of dot spin  $dS^z/dt$ . (b) Two components  $J_{out,in}^z(t)$  contained in  $J^z(t)$ . The vertical lines indicate the duration of the excitation pulse. The parameters used in the calculation are  $\omega = \omega_0 = 50$  and  $\omega_1 = 10$ .

FIG. 4

(Color online) Time-dependent spin current  $J^z(t)$  as a function of temperature  $T$ . The excitation pulse length is set at  $\tau = 6$ . The parameters used in the calculation are  $\omega = \omega_0 = 50$  and  $\omega_1 = 10$ .

FIG. 5

(Color online) Time-dependent spin current  $J^z(t)$  and its two components  $J_{out,in}^z(t)$  at  $T=100$ . The vertical lines indicate the duration of the excitation pulse. The parameters used in the calculation are  $\omega = \omega_0 = 50$  and  $\omega_1 = 10$ .

FIG. A.1

(Color online) (a) Diagonal elements of density matrix  $\rho_{00}(t)$ ,  $\rho_{\uparrow\uparrow}(t)$  and  $\rho_{\downarrow\downarrow}(t)$ . (b) Charge and spin currents  $J^c(t)$  and  $J^z(t)$ . The vertical lines indicate the duration of the excitation pulse. In the calculation,  $\omega = \omega_0 = 50$ ,  $\omega_1 = 10$  and  $U = \infty$  are assumed.

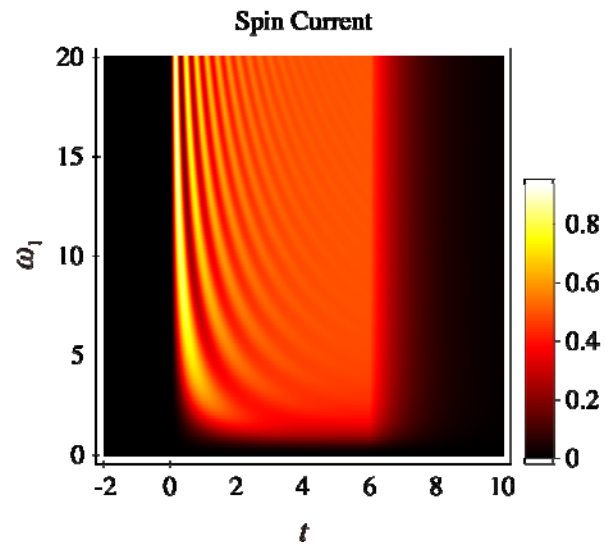


FIG. 1

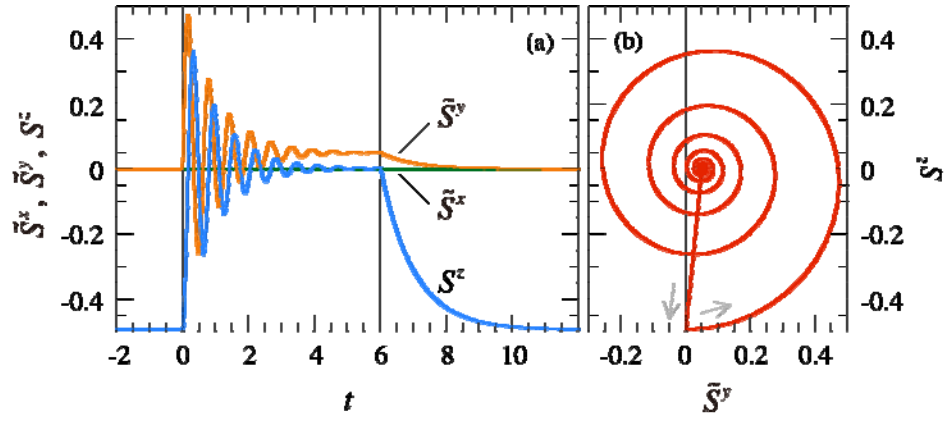


FIG. 2

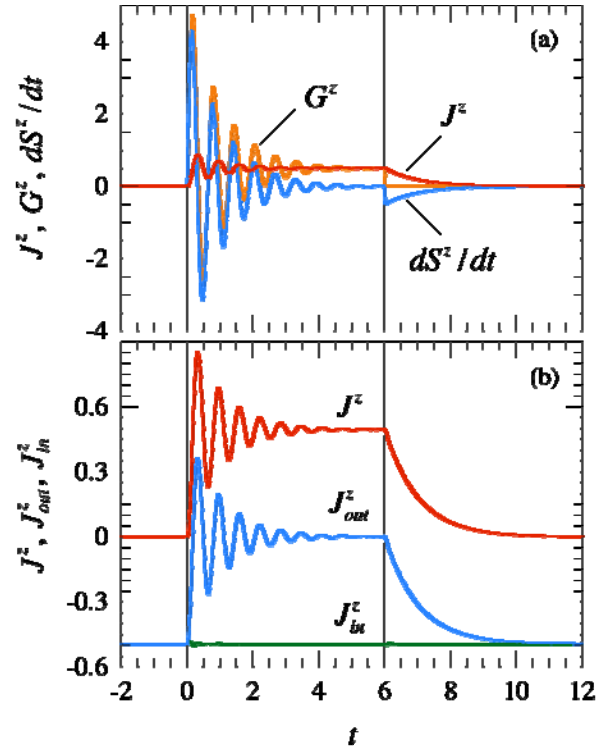


FIG. 3

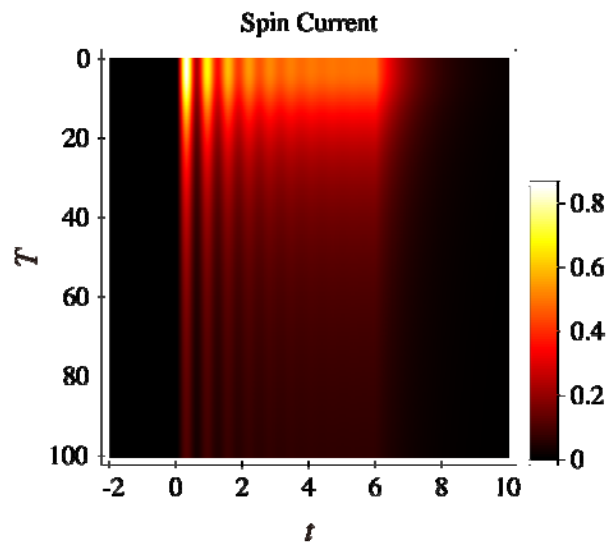


FIG. 4



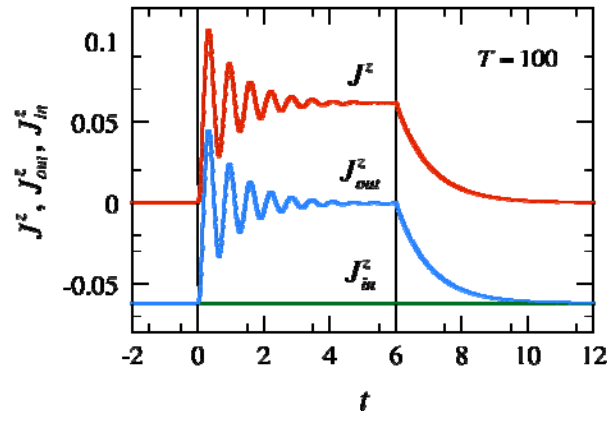


FIG. 5

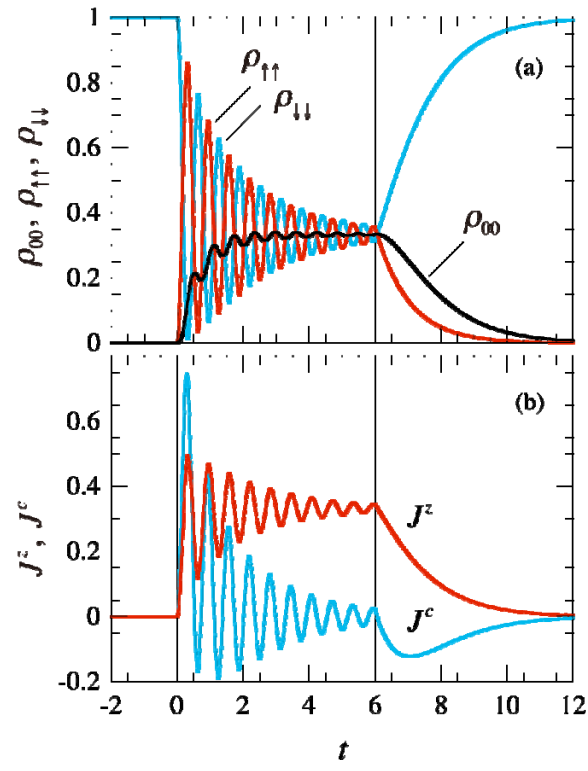


FIG. A.1